

# The winds of O-stars

## II. The terminal velocities of stellar winds of O-type stars

M.A.T. Groenewegen<sup>1</sup>, H.J.G.L.M. Lamers<sup>1,2,3</sup>, and A.W.A. Pauldrach<sup>4</sup>

<sup>1</sup> SRON Laboratory for Space Research, Beneluxlaan 21, NL-3527 HS Utrecht, The Netherlands

<sup>2</sup> Astronomical Institute at Utrecht, Princetonplein 5, NL-3584 CC Utrecht, The Netherlands

<sup>3</sup> Joint Institute for Laboratory Astrophysics, University of Colorado and National Bureau of Standards, Boulder, CO 80309-0440, USA

<sup>4</sup> Universitäts-Sternwarte München, Scheinerstrasse 1, D-8000 München 80, Federal Republic of Germany

Received November 25, 1988; accepted January 25, 1989

**Summary.** The P Cygni profiles of the UV resonance lines of C IV, N V, Si IV and of the subordinate UV lines of N IV and C III, observed in the spectra of 27 O-type stars, are analyzed in detail with the SEI-method. The theoretical profiles which include the effect of turbulence agree very well with the observations and can explain the shape of the violet absorption wings, the deep absorption troughs and the wavelength of the emission peak. The terminal velocities of the stellar winds are derived from a comparison between predicted and observed profiles.

The resulting terminal velocities,  $v_\infty$ , are systematically lower than previous estimates based on profile calculations with the Sobolev method by about  $400 \text{ km s}^{-1}$ . The ratio between the terminal and the escape velocity is  $v_\infty/v_{\text{esc}} = 2.78 \pm 0.36$ . The observed terminal velocities are compared with predicted values for radiation driven winds in which non-LTE effects and multiline scattering is taken into account. The predicted values are systematically higher than the observed ones by 40 percent, independent of luminosity class. Several possibilities for the origin of this discrepancy in terms of uncertain stellar parameter or errors in the predictions of the radiation driven winds are discussed. Either the stellar masses derived from the evolutionary tracks are too high by about 40 percent, or the values of the force multiplier parameters  $\alpha$  and  $\delta$  are not correctly predicted by the present non-LTE wind models.

The reduction of the observed terminal velocities of the winds by about  $400 \text{ km s}^{-1}$  compared to previous estimates implies that the narrow absorption components, observed in the UV resonance lines of O and B stars, reach the terminal velocity of the winds.

**Key words:** circumstellar matter – early-type stars – line profiles – mass loss – turbulence

### 1. Introduction

The winds from early-type stars are accelerated from a small and subsonic velocity at the photosphere to highly supersonic values

---

Send offprint requests to: H.J.G.L.M. Lamers (SRON Laboratory for Space Research)

on the order of  $10^3 \text{ km s}^{-1}$  at large distances. The terminal velocity of the wind, i.e., the velocity reached at “infinity” is one of the most directly measurable quantities of the stellar winds, as it is related to the Doppler shift of the short-wavelength edge of strong UV resonance lines. Early observations suggested that the terminal velocity,  $v_\infty$ , is proportional to the escape velocity at the photosphere,  $v_{\text{esc}}$ , with a ratio  $v_\infty/v_{\text{esc}} = 3$  (Lamers et al., 1976; Snow and Morton, 1976). Later observations of many more stars have shown that this ratio depends on the effective temperature of the star and decreases from a value between 2.5 and 3.5 for  $T_{\text{eff}} \geq 3 \cdot 10^4 \text{ K}$  to about 1 at  $T_{\text{eff}} = 1 \cdot 10^4 \text{ K}$  (Abbott, 1982; Cassinelli and Lamers, 1987).

The theory of radiation driven winds from Castor et al. (1975) and Abbott (1982) predicts a linear relation between  $v_\infty$  and  $v_{\text{esc}}$  with a ratio of about 1 which is smaller than observed. The improvements to this theory by Pauldrach et al. (1986) show a more complex relation between  $v_\infty$  and  $v_{\text{esc}}$ . This predicted relation seems to be confirmed by the comparison between observed and theoretical values of  $v_\infty$  for seven stars selected by Pauldrach et al.

The existence of a well defined relation between  $v_\infty$  and  $v_{\text{esc}}$  has very important consequences because in principle it enables the determination of the surface gravity of the star and of its mass, if the radius is known, from a simple measurement of the edge velocity of the UV resonance lines. However, the accurate determination of the terminal velocity of the stellar winds from the profiles of the UV to resonance lines is not as trivial as generally adopted.

If the velocity law of the stellar wind is a monotonically increasing function of distance from the star, and if the thermal and turbulent velocities can be neglected (as assumed in the Sobolev approximation) the terminal velocity,  $v_\infty$ , is equal to the edge velocity,  $v_{\text{edge}}$ , where the blue wing of the saturated P Cygni profiles reach the continuum. However, accurate comparisons between observed and predicted profiles of UV resonance lines show that some broadening mechanism with a typical velocity of a few hundred  $\text{km s}^{-1}$  is affecting the line formation in the winds of hot stars. Lamers and Rogerson (1978) have argued that the profiles of the O VI lines in the spectrum of  $\tau$  Sco (B0 V) can only be explained by assuming a “turbulent” velocity component with a Doppler width of  $150 \text{ km s}^{-1}$  in the lower wind region. Puls (1987) showed that a turbulent velocity of about  $200 \text{ km s}^{-1}$  is

required to match the observed UV line profiles of  $\zeta$  Pup (O4 If) with the line profiles predicted with the Comoving Frame Method. Such a “turbulence” in the wind can account for the fact that the violet absorption edges of the saturated UV line profiles are not vertical as predicted in the Sobolev approximation (e.g. Castor and Lamers, 1979) but approach the continuum gradually. Lucy (1983, 1984) has proposed that the deep absorption troughs in the observed UV resonance lines of many stars are due to a non-monotonic velocity law, in which shocks are superimposed on a flow velocity which gradually increases outwards. These shocks affect the formation of the UV resonance lines in a way very similar to turbulence. These conclusions imply that the terminal velocities of the winds of O-stars which are derived from the edge velocity of the UV resonance lines or by linefitting with the Sobolev method may be seriously wrong.

Recent calculations of the line profiles of UV resonance lines with the SEI-method (Lamers et al., 1987) have shown that the inclusion of “turbulence” in the profile calculations produces a shift of the violet absorption edge of saturated lines to wavelengths shorter than predicted by the Sobolev theory by about  $2 V_D$ , where  $V_D$  is the velocity of the adopted Gaussian turbulence. Detailed studies of UV lineprofiles reported in this paper show that the “turbulent” velocity in the winds of O-stars is typically on the order of 120 to 350 km s<sup>-1</sup>. This implies that the terminal velocities derived from the edge velocity of the UV resonance line are generally overestimated by several hundreds km s<sup>-1</sup>.

In this paper we will discuss the terminal velocities derived from a detailed comparison between the observed profiles of UV resonance lines of 27 O-stars with predicted profiles. The theoretical profiles are calculated with the SEI-method (Lamers et al., 1987) in which turbulence is allowed for. The details of the linefitting and the results in terms of ionization and mass loss will be described by Groenewegen and Lamers (1989, Paper I). The

values of  $v_\infty$  are compared with previous determinations in Sect. 4, and compared with predictions from the radiation driven wind theory in Sect. 5.

## 2. The observations

For this study we selected 27 O-stars from the Atlas of High Resolution IUE Spectra by Walborn et al. (1985). Both the printed and the magnetic tape version were used. This atlas contains the high resolution IUE spectra of 98 stars in the wavelength range of 1200 to 1900 Å with a resolution of 0.25 Å, corresponding to 50 km s<sup>-1</sup> at 1500 Å. The 27 stars selected cover a range in spectral type from O4 to B0; and luminosity classes from Ia to V. The stars are listed in Table 1 together with their basic parameters. The spectral types are from Walborn et al. (1985). These agree very well with those in the catalogue of Garmany (1987), which is an updated version of the list published by Garmany et al. (1982). The three exceptions are HD101190 (O6 III instead of O6 V (f)), HD188001 (O8 I instead of O7.5 Iaf) and HD 37742 (O9.5 Ib instead of O9.7 Ib). We have kept Walborn's classification, except for HD 37742 for which Garmany's classification agrees very well with the recent study of this star by Voels et al. (1988). For the absolute visual magnitudes we have chosen the values derived from cluster membership, rather than the calibration of  $M_V$  versus spectral type. This choice is based on the consideration that the assignment of a luminosity class to an O-star is sometimes difficult and not always unique. As a result of this, we found that the difference in  $M_V$  between two stars is not always in agreement with their difference in luminosity class. For instance HD 14947 is fainter than HD 15558 although the first one is a supergiant and the second one has a luminosity class III. The adopted absolute visual magnitudes are from the catalogue of Garmany (1987) which is largely based on cluster distances by Humphreys (1978). For HD 37742 ( $\zeta$  Ori A) we have

**Table 1.** The program stars

| HD                           | Name           | Type             | $M_V$ | $\log T_{\text{eff}}$ | $\log L$ | $\log R$ | $\log M$ | $\tau$ | $v_{\text{esc}}$<br>(km/s) | $v_{\text{edge}}$<br>(km/s) | $v_\infty$<br>(km/s) | $v_{\text{turb}}$<br>(km/s) | $v_{\text{edge}}/v_\infty$ | $v_{\text{turb}}/v_\infty$ | $v_\infty/v_{\text{esc}}$ |
|------------------------------|----------------|------------------|-------|-----------------------|----------|----------|----------|--------|----------------------------|-----------------------------|----------------------|-----------------------------|----------------------------|----------------------------|---------------------------|
| 93250                        |                | O3 V ((f))       | -6.1  | 4.686                 | 6.08     | 1.19     | 1.92     | 0.38   | 1120                       | 3700                        | 3300±200             | 260±80                      | 1.12±0.07                  | 0.08±0.05                  | 2.9±0.4                   |
| 93129A                       |                | O3 I f*          | -6.5  | 4.648                 | 6.13     | 1.29     | 1.92     | 0.43   | 960                        | 4240:                       | 3050±60              | 180±80                      | 1.4:                       | 0.06±0.03                  | 3.2±0.4                   |
| 46223                        |                | O4 V ((f))       | -5.3  | 4.667                 | 5.70     | 1.04     | 1.73     | 0.25   | 1190                       | 3190                        | 2800±60              | 200±90                      | 1.14±0.03                  | 0.07±0.03                  | 2.4±0.3                   |
| 164794                       | 9 Sgr          | O4 V ((f))       | -6.1  | 4.667                 | 6.02     | 1.20     | 1.87     | 0.38   | 1060                       | 3440                        | 2950±150             | 210±60                      | 1.17±0.07                  | 0.07±0.02                  | 2.8±0.3                   |
| 66811                        | $\zeta$ Pup    | O4 I (n) f       | -6.0  | 4.627                 | 5.87     | 1.20     | 1.77     | 0.33   | 970                        | 2660                        | 2200±60              | 290±70                      | 1.21±0.04                  | 0.13±0.03                  | 2.3±0.2                   |
| 190429A                      |                | O4 I f+          | -6.4  | 4.627                 | 6.03     | 1.28     | 1.85     | 0.40   | 920                        | 2730                        | 2300±70              | 370±140                     | 1.19±0.03                  | 0.16±0.06                  | 2.5±0.3                   |
| 15629                        |                | O5 V ((f))       | -5.5  | 4.646                 | 5.72     | 1.09     | 1.72     | 0.27   | 1090                       | 3260                        | 2900±70              | 150±80                      | 1.12±0.03                  | 0.05±0.03                  | 2.7±0.3                   |
| 46150                        |                | O5 V ((f))       | -5.5  | 4.646                 | 5.72     | 1.09     | 1.72     | 0.27   | 1090                       | 3170                        | 2900±200             | 200±90                      | 1.09±0.08                  | 0.07±0.03                  | 2.7±0.5                   |
| 93204                        |                | O5 V ((f))       | -4.9  | 4.646                 | 5.48     | 0.97     | 1.62     | 0.19   | 1170                       | 3340                        | 2800±60              | 360±80                      | 1.19±0.03                  | 0.13±0.03                  | 2.4±0.3                   |
| 15558                        |                | O5 III (f)       | -6.4  | 4.626                 | 6.03     | 1.29     | 1.85     | 0.40   | 910                        | 3560                        | 3350±200             | 110±90                      | 1.06±0.07                  | 0.03±0.03                  | 3.6±0.5                   |
| 14947                        |                | O5 I f+          | -6.1  | 4.605                 | 5.85     | 1.24     | 1.74     | 0.34   | 890                        | 2890                        | 2300±70              | 230±100                     | 1.26±0.03                  | 0.10±0.04                  | 2.6±0.3                   |
| 101190                       |                | O5 V ((f))       | -5.7  | 4.625                 | 5.74     | 1.14     | 1.71     | 0.28   | 1010                       | 3260                        | 2900±150             | 170±80                      | 1.12±0.07                  | 0.06±0.03                  | 2.9±0.4                   |
| 210839                       | $\lambda$ Cep  | O6 I nfp         | -6.3  | 4.582                 | 5.87     | 1.29     | 1.75     | 0.35   | 850                        | 2560                        | 2100±60              | 210±70                      | 1.22±0.03                  | 0.10±0.04                  | 2.5±0.3                   |
| 101436                       |                | O6.5 V           | -5.4  | 4.615                 | 5.60     | 1.09     | 1.64     | 0.24   | 1010                       | 3310                        | 2800±150             | 220±80                      | 1.18±0.06                  | 0.08±0.03                  | 2.8±0.4                   |
| 190864                       |                | O6.5 III (f)     | -5.6  | 4.593                 | 5.62     | 1.15     | 1.62     | 0.27   | 910                        | 2810                        | 2450±150             | 125±100                     | 1.15±0.07                  | 0.05±0.04                  | 2.7±0.4                   |
| 163758                       |                | O6.5 Iaf         | -6.6  | 4.571                 | 5.96     | 1.36     | 1.77     | 0.41   | 760                        | 2770                        | 2200±70              | 260±140                     | 1.26±0.04                  | 0.12±0.06                  | 2.9±0.3                   |
| 47839                        | 15 Mon         | O7 V ((f))       | -4.7  | 4.603                 | 5.29     | 0.96     | 1.54     | 0.15   | 1110                       | 3060:                       | 2300±200             | 320±110                     | 1.3:                       | 0.14±0.05                  | 2.1±0.4                   |
| 24912                        | $\epsilon$ Per | O7.5 III(n)((f)) | -5.0  | 4.569                 | 5.32     | 1.04     | 1.50     | 0.18   | 950                        | 3000                        | 2400±100             | 290±120                     | 1.25±0.05                  | 0.12±0.05                  | 2.5±0.3                   |
| 188001                       | 9 Sge          | O7.5 Iaf         | -6.6  | 4.545                 | 5.90     | 1.38     | 1.72     | 0.40   | 710                        | 1900                        | 1800±70              | 250±90                      | 1.06±0.04                  | 0.14±0.05                  | 2.5±0.3                   |
| 101413                       |                | O8 V             | -4.7  | 4.580                 | 5.23     | 1.12     | 1.48     | 0.15   | 860                        | 3370                        | 2900±200             | 580±290                     | 1.16±0.09                  | 0.20±0.10                  | 3.4±0.7                   |
| 36861                        | $\lambda$ Ori  | O8 III ((f))     | -5.2  | 4.556                 | 5.36     | 1.09     | 1.51     | 0.19   | 900                        | 2700                        | 2400±150             | 290±70                      | 1.13±0.07                  | 0.12±0.03                  | 2.7±0.4                   |
| 151804                       |                | O8 Iaf           | -7.3  | 4.532                 | 6.14     | 1.53     | 1.84     | 0.53   | 600                        | 1710                        | 1600±70              | 240±80                      | 1.07±0.04                  | 0.15±0.05                  | 2.7±0.9                   |
| 37043                        | $\nu$ Ori      | O9 III           | -5.9  | 4.532                 | 5.58     | 1.25     | 1.59     | 0.26   | 790                        | 2360                        | 2450±150             | 370±70                      | 0.96±0.07                  | 0.15±0.03                  | 3.1±0.4                   |
| 30614                        | $\alpha$ Cam   | O9.5 Ia          | -7.1  | 4.490                 | 5.95     | 1.52     | 1.71     | 0.46   | 560                        | 1890                        | 1550±60              | 190±60                      | 1.22±0.05                  | 0.12±0.04                  | 3.4±0.4                   |
| 37742                        | $\zeta$ Ori    | O9.7 Ib          | -6.6  | 4.484                 | 5.74     | 1.42     | 1.61     | 0.36   | 620                        | 2290                        | 2100±150             | 320±130                     | 1.09±0.08                  | 0.15±0.06                  | 3.4±0.6                   |
| 149038                       | $\mu$ Nor      | O9.7 Iab         | -6.5  | 4.484                 | 5.70     | 1.40     | 1.58     | 0.35   | 610                        | 2190                        | 1750±100             | 260±150                     | 1.25±0.07                  | 0.15±0.08                  | 2.9±0.4                   |
| 37128                        | $\epsilon$ Ori | B0 Ia            | -7.0  | 4.447                 | 5.80     | 1.53     | 1.62     | 0.40   | 530                        | 2010                        | 1500±150             | 230±80                      | 1.34±0.13                  | 0.15±0.05                  | 2.8±0.4                   |
| Typical uncertainties: (dex) |                |                  | 0.5   | 0.02                  | 0.2      | 0.14     | 0.10     | 0.10   | 0.15                       |                             |                      |                             |                            |                            |                           |

increased the absolute visual magnitude of  $M_V = -6.9$  to  $-6.6$ , to allow for the fact that  $\zeta$  Ori A is a triple with both companions two magnitudes fainter than the primary. For HD 30614 ( $\alpha$  Cam) and HD 149038 ( $\mu$  Nor) which are not a member of a cluster we adopted the values of  $M_V = -7.1$  and  $-6.5$  respectively from the calibration by Humphreys and McElroy (1984). The values of  $T_{\text{eff}}$  and  $L$  are derived from the relations between  $T_{\text{eff}}$ , B.C. and spectral types from Chlebowski and Garmany (1988). These relations are based on a critical compilation of  $T_{\text{eff}}$  and B.C.-values from published non-LTE analyses of O-stars by various groups. For HD 37128 ( $\varepsilon$  Ori) we adopted the values of  $M_V$  from Humphreys (1978) and the values of  $T_{\text{eff}}$  and B.C. from Humphreys and McElroy (1984). The values in Table 1 have an estimated uncertainty of  $\Delta \log T_{\text{eff}} \approx \pm 0.02$  and  $\Delta \log L \approx \pm 0.2$ . The stellar radii are derived from  $L$  and  $T_{\text{eff}}$ , so  $\Delta \log R \approx \pm 0.14$ .

The stellar masses are derived from their location in the HR diagram. We adopted the evolutionary tracks from Maeder and Meynet (1987). In these evolutionary calculations the effects of mass loss and convective overshooting are taken into account. The overshooting parameter is chosen in such a way that the evolution tracks reproduce the observed width of the main sequence for young clusters and associations. These evolution models predict the correct upper limit for the luminosity of red supergiants and the ratio of the lifetimes of the WC and WN stars. We assumed that all the O-stars are in the Hydrogen core-burning phase, i.e., they are moving away from the ZAMS. For stars with  $\log L \gtrsim 5.5$  this assumption might not be valid, as the evolutionary calculations show that the stars with an initial mass of  $M_i \gtrsim 40 M_\odot$  cross the main-sequence region of the HR diagram a second time when they are evolving to the left to become a Wolf-Rayet star. During this second crossing the mass, corresponding to a certain luminosity, is typically half as large as during the first crossing. We will return to this problem in Sect. 6.

The masses listed in Table 1 have an uncertainty of about 0.1 dex, which is mainly due to the uncertainty in  $L$  of 0.2 dex.

The effective escape velocity is

$$v_{\text{esc}} = \{2 GM(1 - \Gamma)/R\}^{0.5} \quad (1)$$

with

$$\Gamma = 7.66 \cdot 10^{-5} \sigma_e (L/L_\odot) (M/M_\odot)^{-1} \quad (2)$$

and  $\sigma_e = 0.347$  for an atmosphere of a Population I star in which both H and He are fully ionized. The values of  $\Gamma$  and  $v_{\text{esc}}$  are given in Table 1. The uncertainty of  $\Gamma$  is about 0.1 dex or 25% because the uncertainty of  $\Delta \log L = 0.2$  is partly compensated by the corresponding error of  $\Delta \log M = 0.1$ . The values of  $v_{\text{esc}}$  have a typical uncertainty of 10% if  $\Gamma \lesssim 0.4$  and 15% if  $\Gamma \approx 0.5$ . The largest uncertainty in  $v_{\text{esc}}$  is reached by HD 151804 which has an uncertainty of  $v_{\text{esc}}$  of 17%. The small uncertainty in  $v_{\text{esc}}$ , in spite of the large uncertainty of  $\Delta \log R = 0.14$ , is due to the fact that the errors in  $M$  and  $R$  cancel one another because  $M \sim L^{1/2}$  and  $R \sim L^{1/2} T^{-2}$  so  $v_{\text{esc}} \sim T$ . All these errors indicate the possible deviations from the values listed in Table 1, due to  $\Delta \log L = 0.2$  and  $\Delta \log T_{\text{eff}} = 0.02$ . The quoted errors are not standard deviations.

The errors are calculated under the assumption that the relation between the stellar mass and its  $T_{\text{eff}}$  and  $L$  is accurately defined. The effects of the uncertainties in the evolutionary masses will be discussed later.

The edge velocities, i.e., the velocity at which the violet absorption edge of the strongest UV resonance line (usually C IV)

reaches the continuum, is listed in Table 1, column 11. These values are taken from Abbott (1978), based on Copernicus-spectra and supplemented with our own determinations based on the IUE spectra in the Atlas of High Resolution IUE Spectra (Walborn et al., 1985). The edge velocities have an estimated accuracy on the order of  $100 \text{ km s}^{-1}$ .

### 3. The linefits

The observed profiles of the UV resonance lines of C IV  $\lambda\lambda 1548.188$  and  $1550.762$ , N V  $\lambda\lambda 1238.808$  and  $1242.796$  and Si IV  $\lambda\lambda 1393.755$  and  $1402.770$  and of the subordinate lines of N IV  $\lambda 1718.55$  and C III  $\lambda\lambda 1174.930 - 1176.370$  (six lines) are fitted with the theoretical profiles calculated with the SEI-method (Lamers et al., 1987). In this method the source function of the lines is calculated in the Sobolev approximation, but the equation of transfer is solved exactly. For doublet lines the radiative coupling between the components is allowed for. This method, suggested by Hamann (1981), produces line profiles which are very similar to those calculated with the physically more correct Comoving Frame Method, but in a simpler and faster way.

The fitting of the line profiles requires the following input: the velocity law  $v(r)$  and the optical depth law  $\tau(v)$ . The effect of turbulence in the stellar wind can be taken into account. The details of the linefitting procedure are described in a forthcoming paper (Groenewegen and Lamers, 1989). For this study the relevant fit parameters are the terminal velocity  $v_\infty$  and the turbulent velocity  $v_{\text{turb}}$ . The velocity law is characterized by

$$w(x) = w_0 + (1 - w_0)(1 - 1/x)^\beta \quad (3)$$

with  $w = v/v_\infty$ ,  $x = r/R_*$  and  $w_0 = v(R_*)/v_\infty$ . The fit parameters are  $\beta$ , which describes the steepness of the velocity law, and  $v_\infty$ . For the initial velocity of the stellar wind a value of  $w_0 = 0.01$  was adopted. The turbulence is assumed to be Gaussian with a depth-independent velocity of  $v_{\text{turb}}$ .

Typical fits of the observed profiles with predicted profiles of resonance lines are shown in Fig. 1 for the star  $\lambda$  Cep. This figure shows the accuracy of the linefits which can be obtained. The location of the wavelength which correspond to the terminal velocity  $v_\infty = 2100 \text{ km s}^{-1}$  of this star, is indicated. Figure 1 shows that the terminal velocity is considerably smaller than the velocity indicated by the violet edge of the profiles. The difference of about  $450 \text{ km s}^{-1}$  is due to the effect of turbulence in the wind with  $v_{\text{turb}} = 210 \text{ km s}^{-1}$ . The effect of turbulence is also noticeable in the wavelengths of the maximum emission. In the Sobolev approximation this maximum occurs at the rest wavelength of the red component of the doublet. In the case of a turbulent wind however, this maximum shifts to longer wavelengths by about  $\Delta\lambda = 2v_{\text{turb}}(\lambda/c)$ , in agreement with the observations.

### 4. The terminal and turbulent velocities

The terminal velocities derived from the linefits are listed in Table 1, column 12. The estimated accuracy of  $v_\infty$  is derived on the basis of two criteria: the saturation of the strongest lines (higher saturation yields more reliable values of  $v_\infty$ ), and the accuracy of the linefits. The best determinations of  $v_\infty$  have an accuracy of about  $60 \text{ km s}^{-1}$ . The lower limit to the accuracy is determined by the resolution of IUE.

The turbulent velocities derived from the linefits are listed in Table 1, column 13. The uncertainty is estimated on the basis of

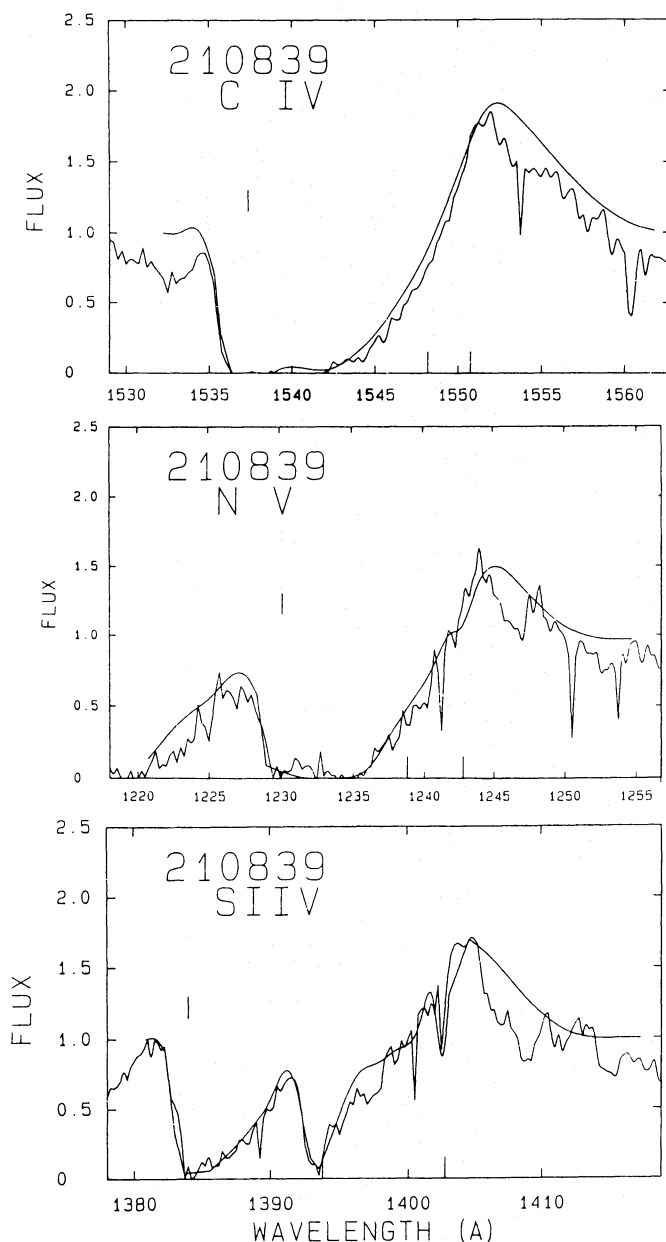


**Fig. 1.** The observed and predicted profiles of the resonance lines of C IV, N v and Si IV of the star  $\lambda$  Cep (HD 210839). The effect of the interstellar  $\text{L}\alpha$  line with a column density of  $N_{\text{HI}} = 1.2 \cdot 10^{21} \text{ cm}^{-2}$  on the profile of the N v doublet is taken into account. Notice that the line fits predict the correct width of the deep absorptions of the C IV and N v lines, the correct location of the emission peak and the correct shape of the violet absorption edges. The wavelength corresponding to  $v_{\infty}$  is indicated by a vertical line

the linefits for all the lines, given in Sect. 3, with a minimum uncertainty of  $60 \text{ km s}^{-1}$ . The last three columns of Table 1 show the values of ratios  $v_{\text{edge}}/v_{\infty}$ ,  $v_{\text{turb}}/v_{\infty}$  and  $v_{\infty}/v_{\text{esc}}$ .

#### 4.1. Comparison with other determinations of $v_{\infty}$

The values of  $v_{\infty}$  determined in this study are systematically lower than those derived from the edge velocities of the UV resonance

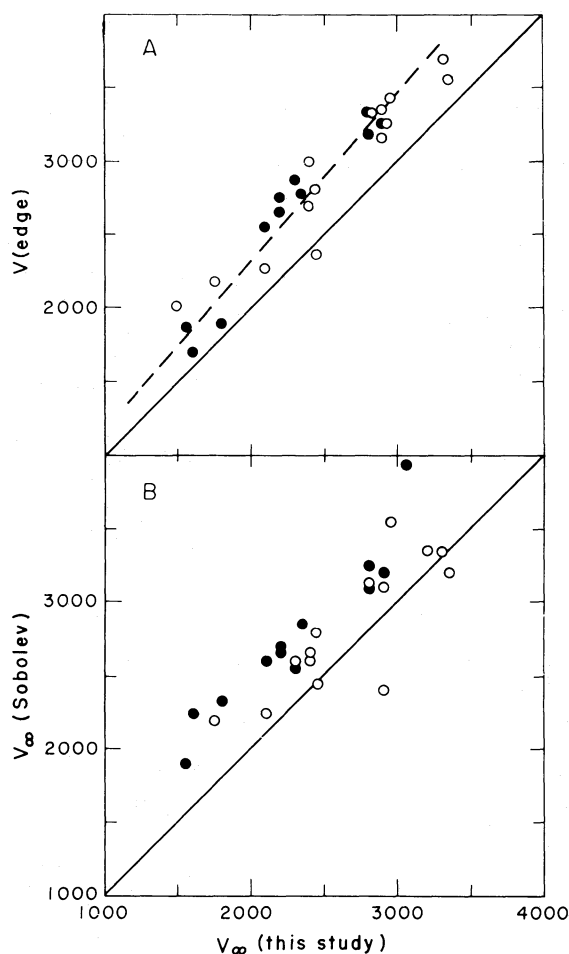


**Fig. 2A and B.** Comparison between the edge-velocity of the UV resonance lines (A), and the terminal velocities derived by fitting with lines in the Sobolev approximation (B) with our results. Filled symbols refer to most accurate values of  $\Delta v_{\infty} \leq 70 \text{ km s}^{-1}$ . Notice that  $v_{\text{edge}}$  and  $v_{\infty}$  (Sobolev) are about  $400 \text{ km s}^{-1}$  larger than our determinations of  $v_{\infty}$ . The dashed line in A represents Eq. (4)

lines or from line profile fitting with the Sobolev-method. This is shown in Fig. 2B, where the values of  $v_{\infty}$  derived from linefits calculated with the escape probability method in the Sobolev approximation by Howarth and Prinja (1988) are compared with our results. The data in this figure show that the velocities derived from the fits with Sobolev-profiles are systematically too high by about  $400 \text{ km s}^{-1}$ . This effect was already noticed in Sect. 3 (Fig. 1).

The UV line profiles of the star  $\zeta$  Pup (O4 If) were studied by Hamann (1980) using the Comoving Frame Method with turbulence taken into account. He found a terminal velocity of  $2400 \text{ km s}^{-1}$  for this star, which is higher than our value of  $2200 \text{ km s}^{-1}$ . The difference is due to the fact that Hamann adopted an arbitrary value of  $v_{\text{turb}} = 100 \text{ km s}^{-1}$ , whereas we found from the linefits that  $v_{\text{turb}} = 290 \pm 30 \text{ km s}^{-1}$ . A close inspection of the linefits obtained by Hamann and by us shows that our fits match the observations better than Hamann's fits. In particular the wide absorption troughs of the C IV and N v resonance lines, which are very sensitive to the turbulent velocity, are matched better by our linefits. This indicates that Hamann's



adopted value of  $v_{\text{turb}} = 100 \text{ km s}^{-1}$  is an underestimate, and consequently his value of  $v_{\infty} = 2400 \text{ km s}^{-1}$  will be an overestimate.

Our value of  $v_{\infty} = 2200 \text{ km s}^{-1}$  for the star  $\zeta$  Pup agrees very well with the value of  $v_{\infty} = 2140$  to  $2200 \text{ km s}^{-1}$  derived from non-LTE linefits including turbulence by Puls (1987).

#### 4.2. The relation between $v_{\text{edge}}$ and $v_{\infty}$

The values of  $v_{\text{edge}}$  are compared with those of  $v_{\infty}$  in Fig. 2A. The figure shows that  $v_{\text{edge}}$  is higher than  $v_{\infty}$  by about  $400 \text{ km s}^{-1}$ . The dashed line in this figure shows a mean relation which is forced through the point  $v_{\text{edge}} = v_{\infty} = 0 \text{ km s}^{-1}$ . This relation is of the form

$$v_{\text{edge}} \simeq (1.15 \pm 0.06) v_{\infty} \quad (4)$$

or

$$v_{\infty} \simeq (0.87 \pm 0.05) v_{\text{edge}} \quad (5)$$

#### 4.3. The relation between $v_{\infty}$ and $v_{\text{esc}}$

The relation between  $v_{\infty}$  and  $v_{\text{esc}}$  is plotted in Fig. 3. Different symbols refer to different luminosity classes. We have not indicated the error bars in this figure. The stars with  $\Delta v_{\infty} < 100 \text{ km s}^{-1}$  are mainly supergiants which have an uncertainty in  $v_{\text{esc}}$  of 10 to 15%. On the other hand, the stars with the most accurate values of  $v_{\text{esc}}$  are main-sequence stars which in general have a larger uncertainty in  $v_{\infty}$ . Typical errors are  $\Delta v_{\infty} \simeq 150 \text{ km s}^{-1}$  and  $\Delta v_{\text{esc}} \simeq 100 \text{ km s}^{-1}$  for luminosity class V stars, and  $\Delta v_{\infty} \simeq 70 \text{ km s}^{-1}$  and  $\Delta v_{\text{esc}} \simeq 120 \text{ km s}^{-1}$  for stars of luminosity class I.

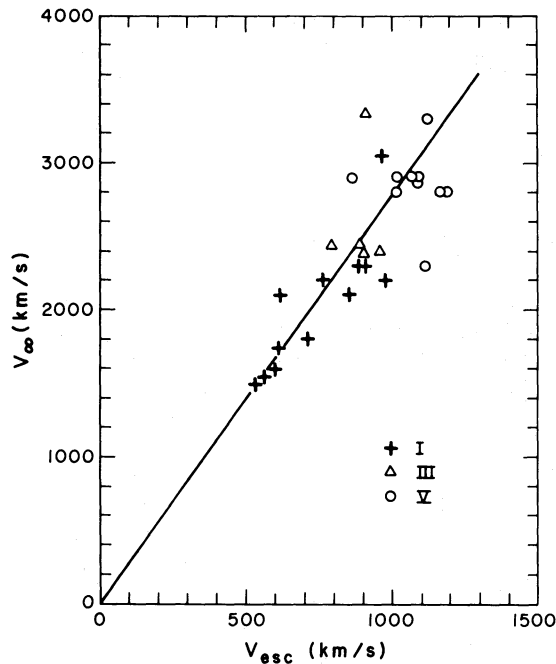


**Fig. 3.** Comparison between  $v_{\infty}$  and  $v_{\text{esc}}$ . Different symbols refer to different luminosity classes. The uncertainties in  $v_{\infty}$  and  $v_{\text{esc}}$  are on the order of  $100 \text{ km s}^{-1}$  (see 4.3). The full line indicates the relation  $v_{\infty} = 2.78 v_{\text{esc}}$  (Eq. 6). The same proportionality factor is found for the different luminosity classes

The mean relation through the data-points which goes through the origin of the graph is

$$v_{\infty} = (2.78 \pm 0.36) v_{\text{esc}}. \quad (6)$$

This relation is quite different from the ones derived by Abbott (1978)

$$v_{\infty} = 540 + 2.4 v_{\text{esc}} \quad (7)$$

and by Prinja (1985)

$$v_{\infty} = 947 + 1.9 v_{\text{esc}}. \quad (8)$$

The difference between our relation and the ones derived by Abbott and Prinja are due to two effects. Firstly, our values of  $v_{\infty}$  are smaller than those derived earlier by about  $400 \text{ km s}^{-1}$  (Sect. 4.1), and secondly we used improved evolutionary tracks by Maeder and Meynet (1987) which include mass loss and convective overshooting, and lead to smaller masses than the tracks of Chiosi et al. (1978) adopted by Abbott. For example, for the star  $\zeta$  Pup Abbott assumed  $v_{\text{esc}} = 1050 \text{ km s}^{-1}$  and  $v_{\infty} = 2660 \text{ km s}^{-1}$ , whereas our values are 970 and  $2200 \text{ km s}^{-1}$  respectively.

Our results show that the constant term of  $540 \text{ km s}^{-1}$  in Abbott's empirical relation is largely due to the systematic overestimate of  $v_{\infty}$ . This is reassuring because one expects on the basis of the radiation driven wind theory that  $v_{\infty}$  is roughly proportional to  $v_{\text{esc}}$ . (A detailed comparison with observed and predicted values of  $v_{\infty}$  is given in Sect. 5.)

The ratio  $v_{\infty}/v_{\text{esc}}$  is plotted versus  $\log T_{\text{eff}}$  in Fig. 4. The data are consistent with a constant ratio of  $v_{\infty}/v_{\text{esc}} = 2.78$ . There is some indication of a decreasing ratio towards higher temperatures:

$$v_{\infty}/v_{\text{esc}} = 2.78 - 3.1 (\log T_{\text{eff}} - 4.60) \quad (9)$$

but this trend is uncertain. Such a trend, which is valid for the O-stars only, was already suggested by Abbott (1982). For B-stars the ratio  $v_{\infty}/v_{\text{esc}}$  decreases with decreasing temperature, reaching  $v_{\infty}/v_{\text{esc}} \simeq 1$  at  $T_{\text{eff}} \simeq 10000 \text{ K}$ .

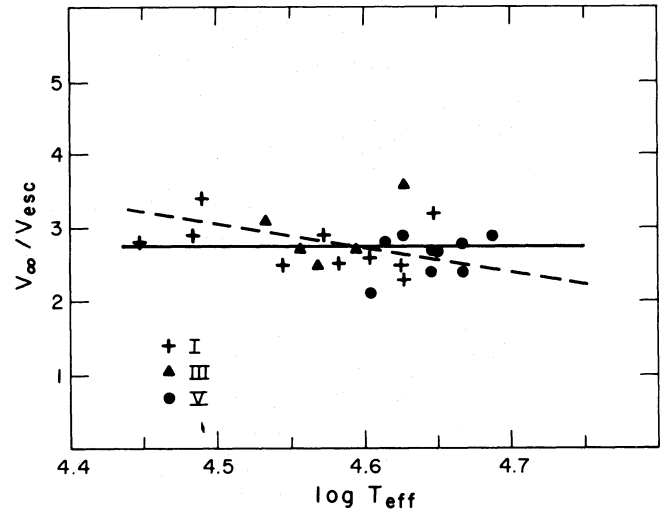


**Fig. 4.** The relation between  $v_{\infty}/v_{\text{esc}}$  and  $T_{\text{eff}}$ . The values of  $v_{\infty}/v_{\text{esc}}$  have an uncertainty of about 0.4. The stars HD 101413 and HD 151804 with  $\Delta(v_{\infty}/v_{\text{esc}}) \geq 0.7$  are omitted. The data are consistent a constant value of  $v_{\infty}/v_{\text{esc}} = 2.78$  (full line), but there is a weak indication of a temperature dependence (dashed line) as in Eq. (9)

#### 4.4. The turbulent velocities

The turbulent velocities  $v_{\text{turb}}$  and the ratio  $v_{\text{turb}}/v_{\infty}$  are plotted versus  $T_{\text{eff}}$  in Fig. 5. The turbulent velocities are in the range of 150 to 300 km s<sup>-1</sup> with a few higher and lower values. This corresponds to  $v_{\text{turb}}/v_{\infty} \approx 0.05$  to 0.10 for stars of types O7 and earlier and  $v_{\text{turb}}/v_{\infty} \approx 0.12$  to 0.16 for the later O-stars. The highest value of  $v_{\text{turb}} = 580 \pm 290$  km s<sup>-1</sup> was found for HD 101413. The linefits of this star, however, have a poor accuracy so the resulting value of  $v_{\text{turb}}$  is very uncertain.

### 5. Comparison between observed and predicted values of $v_{\infty}$

#### 5.1. The predicted values of $v_{\infty}$ for radiation driven winds

The theory of radiation driven stellar winds, first developed quantitatively by Castor et al. (1975), has been improved drastically by Pauldrach et al. (1986) by allowing for the non-radial streaming of photons from the photosphere and by the simultaneous solution of the hydrodynamics and radiative transfer equations in the Comoving Frame Method.

Kudritzki et al. (1988b) have derived analytical solutions for the wind-models. These solutions yield accurate approximations of  $v_{\infty}$  to an accuracy of 5% and  $\dot{M}$  to an accuracy of 10%, when the stellar parameters and the force multiplier parameters  $k$ ,  $\alpha$  and  $\delta$  are known. This approximation for  $v_{\infty}$  will be used here. The predicted values of  $v_{\infty}$  depend strongly on  $\alpha$ , weakly on  $\delta$ , and are independent of  $k$ .

The force multiplier parameters are defined by the following approximations:

$$M(t) = kt^{-\alpha}(n_e/W)^{\delta} \quad (10)$$

where  $M(t)$  is the force multiplier (i.e., the line force in units of the Thomson-scattering force),  $t$  is an optical depth parameter

$$t = \sigma_e \rho v_{\text{th}} (dv/dr)^{-1} \quad (11)$$

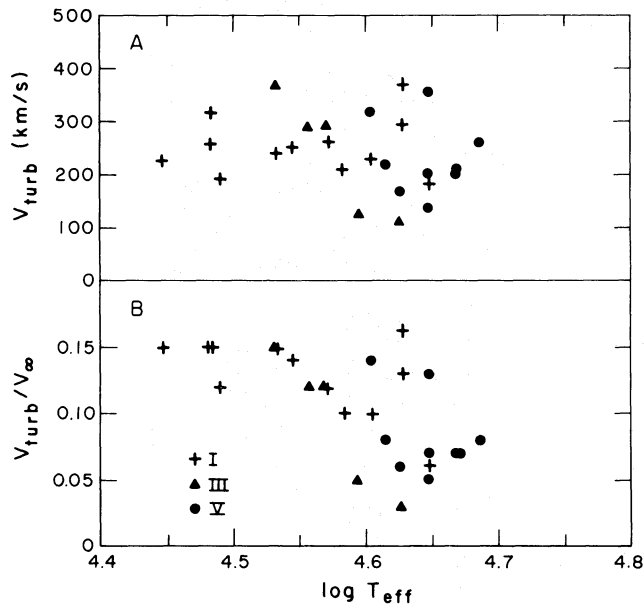


Fig. 5A and B. The relation between  $v_{\text{turb}}$  (A) and  $v_{\text{turb}}/v_{\infty}$  (B) and temperature. Different symbols indicate different luminosity classes. The star HD 101413 with a very uncertain value of  $v_{\text{turb}}$  has been omitted

with  $\sigma_e$  is the Thomson-scattering coefficient per gram,  $v_{\text{th}}$  is the thermal velocity of the carbon ions in the wind,  $dv/dr$  is the velocity gradient in the wind and  $W$  is the geometrical dilution factor (Pauldrach et al., 1986).

The values of  $k$ ,  $\alpha$  and  $\delta$  have been calculated with the assumption of LTE for a large range of models of  $T_{\text{eff}} = 20,000 - 50,000$  K by Abbott (1982) and Pauldrach et al. (1986). The values from the second paper are plotted in Fig. 6 (filled symbols). More recently Pauldrach et al. (1988) have calculated the force multiplier for a grid of models with  $32,000 \leq T_{\text{eff}} \leq 51,000$  K, taking into account non-LTE effects on the level populations and multiline scattering or absorption of photons (see Fig. 6, open symbols). The non-LTE values of  $k$  cluster around  $0.052 \pm 0.012$  which is about twice as small as the LTE-values. The non-LTE values of  $\alpha$  are centered at  $0.695 \pm 0.012$ , except for the coolest model of  $T_{\text{eff}} = 32,000$  which has a value of  $\alpha = 0.737$ . These values of  $\alpha$  are larger than the LTE-values by about  $0.07 \pm 0.02$  except for  $T_{\text{eff}} = 32,000$  K. The non-LTE values of  $\delta$  are centered at  $\delta = 0.072 \pm 0.009$  if  $T_{\text{eff}} \geq 35,500$  K and  $\delta = 0.031 \pm 0.006$  if  $32,000 \leq T_{\text{eff}} < 35,000$  K. These values of  $\delta$  are smaller than the

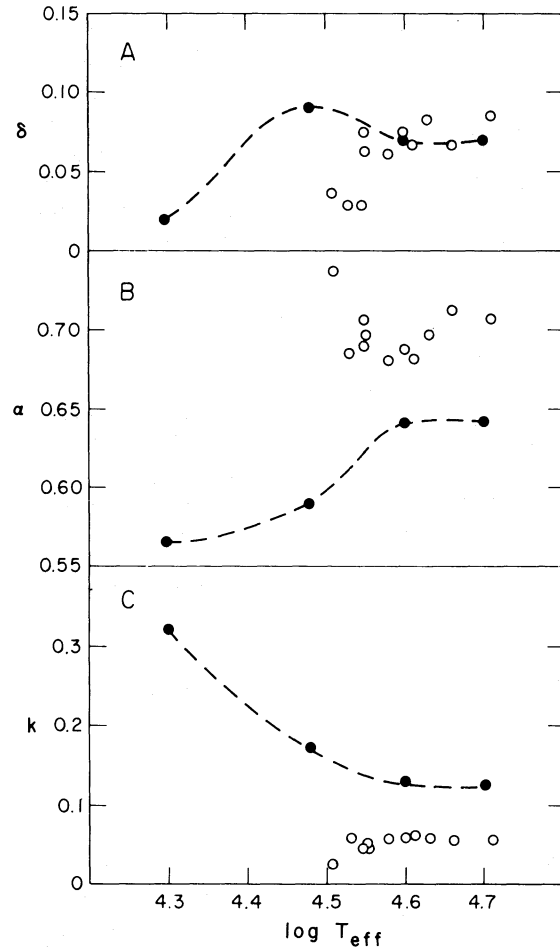


Fig. 6A–C. The predicted values of the force multiplier parameters  $k$ ,  $\alpha$  and  $\delta$  as a function of  $T_{\text{eff}}$ . Filled symbols represent LTE calculations (Pauldrach et al., 1986). Open circles represent non-LTE calculations in which the effect of multiline scattering are taken into account (Pauldrach et al., 1988). The scatter is due to an arbitrary selection of the stellar parameter sets

LTE-values at  $T_{\text{eff}} < 35,000$  K but they agree with the LTE values at higher temperatures.

We adopt the mean values derived from the non-LTE calculations:  $\bar{\alpha} = 0.695$  and  $\bar{\delta} = 0.07$  at  $T_{\text{eff}} \geq 35,000$  K and  $\bar{\delta} = 0.03$  at  $T_{\text{eff}} < 35,000$  K. The values of  $k$  do not enter into the calculations of  $v_{\infty}$ . The sensitivity of the predicted values of  $v_{\infty}$  to the adopted values of  $\alpha$  and  $\delta$  will be discussed below.

We realize that the assumption of one mean value for  $\bar{\alpha}$  and  $\bar{\delta}$  is a severe oversimplification, because the values of the force multipliers depend on the stellar parameters in an intricate way and thus may vary from star to star. Therefore a detailed analysis of the comparison between  $v_{\infty}(\text{obs})$  and  $v_{\infty}(\text{pred})$  on the basis of individual stars will require the calculation of  $k$ ,  $\alpha$  and  $\delta$  for each star separately. Such a study is beyond the scope of this paper. Here we will show the general trends of the relation between  $v_{\infty}(\text{obs})$  and  $v_{\infty}(\text{pred})$ . Since the calculations by Pauldrach et al. (1988) show that in the temperature range of the O-stars and in the gravity range of  $3.2 \leq \log g \leq 4.0$  the values of  $k$ ,  $\alpha$  and  $\delta$  happen to cluster around the adopted mean values with only a small scatter, we feel justified to adopt the mean values for the present purpose of showing these trends.

### 5.2. Comparison between predicted and observed values of $v_{\infty}$

The predicted values of  $v_{\infty}$  are listed in Table 2 and plotted versus the observed values in Fig. 7. The values of  $v_{\infty}(\text{pred})$  are systematically larger than  $v_{\infty}(\text{obs})$  by about 40%. The overestimate does not seem to be related to the luminosity class, as we find about the same factor for class I, III and V stars (see Table 3). We will discuss the origin of the discrepancy in terms of uncertainties in the stellar parameters and in the values of  $\alpha$  and  $\delta$ .

#### 5.2.1. Uncertainties in the stellar parameters

The theory of radiation driven winds predicts that  $v_{\infty}$  depends almost linearly on  $v_{\text{esc}}$ . The uncertainty in  $v_{\text{esc}}$  is about 10% if  $\Gamma < 0.5$  and 15% if  $\Gamma \simeq 0.5$  (Sect. 2) if the evolutionary calculations are correct. A reduction of  $v_{\text{esc}}$  by factor  $(1.4)^{-1} \simeq 0.7$  would reduce the discrepancy between  $v_{\infty}(\text{obs})$  and  $v_{\infty}(\text{pred})$ . Such a reduction could be reached by decreasing the mass or increasing the radius of the star. The size of the change depends on the value of  $\Gamma$ . If  $\Gamma = 0$  then a reduction of  $M$  by a factor 0.5 or an increase of  $R$  by a factor 2 will lower  $v_{\text{esc}}$  by a factor 0.7. However if  $\Gamma = 0.4$

then a reduction of  $M$  by a factor 0.7 will increase  $\Gamma$  to 0.57 and reduce  $v_{\infty}$  by a factor 0.71, if  $L$  is assumed to be constant. If  $\Gamma = 0.2$  then the mass must be reduced by a factor 0.6 to explain the discrepancy. This implies that the evolutionary masses must have been seriously overestimated by a factor between 1.4 and 1.7 if the discrepancy between  $v_{\infty}(\text{pred})$  and  $v_{\infty}(\text{obs})$  is to be blamed on the stellar masses.

The dependence of  $v_{\text{esc}}$  on the stellar parameters can be checked in detail by comparing the results for stars with masses derived from the spectroscopic gravity and from evolutionary tracks. In Table 4 we present the stellar parameters and the resulting values of  $v_{\text{esc}}$  for seven program stars for which the

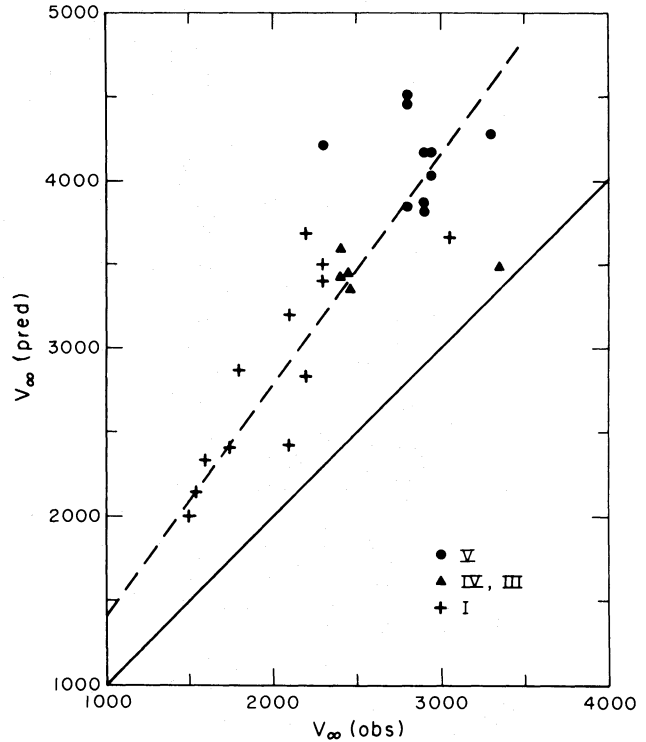


Fig. 7. Comparison between predicted and observed values of  $v_{\infty}$ . Different symbols represent different luminosity classes. The mean relation  $v_{\infty}(\text{pred}) = 1.42 v_{\infty}(\text{obs})$  (see Table 3) is indicated by a dashed line

Table 2. Comparison between observed and predicted values of  $v_{\infty}$

| HD      | $v_{\infty}(\text{obs})$<br>(km s <sup>-1</sup> ) | $v_{\infty}(\text{pred})$<br>(km s <sup>-1</sup> ) | $\frac{v_{\infty}(\text{pred})}{v_{\text{esc}}}$ | HD     | $v_{\infty}(\text{obs})$<br>(km s <sup>-1</sup> ) | $v_{\infty}(\text{pred})$<br>(km s <sup>-1</sup> ) | $\frac{v_{\infty}(\text{pred})}{v_{\text{esc}}}$ | HD     | $v_{\infty}(\text{obs})$<br>(km s <sup>-1</sup> ) | $v_{\infty}(\text{pred})$<br>(km s <sup>-1</sup> ) | $\frac{v_{\infty}(\text{pred})}{v_{\text{esc}}}$ |
|---------|---|--|--|--------|---|--|--|--------|---|--|--|
| 93250   | 3300 ± 200  | 4280   | 3.82   | 15558  | 3350 ± 200  | 3490   | 3.84   | 188001 | 1800 ± 70   | 2870   | 4.04   |
| 93129A  | 3050 ± 60   | 3670   | 3.82   | 14947  | 2300 ± 70   | 3400   | 3.82   | 101413 | 2900 ± 200  | 3860   | 4.49   |
| 46223   | 2800 ± 60   | 4520   | 3.80   | 101190 | 2900 ± 150  | 3820   | 3.78   | 36861  | 2400 ± 150  | 3430   | 3.81   |
| 164794  | 2950 ± 150  | 4030   | 3.80   | 210839 | 2100 ± 60   | 3210   | 3.78   | 151804 | 1600 ± 70   | 2340   | 3.90   |
| 66811   | 2200 ± 60   | 3690   | 3.80   | 101436 | 2800 ± 150  | 3840   | 3.80   | 37043  | 2450 ± 150  | 3350   | 4.24   |
| 190429A | 2300 ± 70   | 3500   | 3.80   | 190864 | 2450 ± 150  | 3470   | 3.81   | 30614  | 1550 ± 60   | 2150   | 3.84   |
| 15629   | 2900 ± 70   | 4160   | 3.82   | 163758 | 2200 ± 70   | 2840   | 3.74   | 37742  | 2100 ± 150  | 2420   | 3.90   |
| 46150   | 2900 ± 200  | 4160   | 3.82   | 47839  | 2300 ± 200  | 4210   | 3.79   | 149038 | 1750 ± 100  | 2400   | 3.93   |
| 93204   | 2800 ± 60   | 4460   | 3.81   | 24912  | 2400 ± 100  | 3600   | 3.79   | 37128  | 1500 ± 150  | 2000   | 3.77   |

parameters were derived independently by means of detailed non-LTE studies of the photospheric spectrum. The parameters and the resulting values of  $v_{\text{esc}}$  are given for our analysis (b) and for the non-LTE analysis (a). In both cases the values of  $L$  are derived from  $M_V$  and B.C. ( $T_{\text{eff}}$ ), with  $T_{\text{eff}}$  derived independently. The uncertainty in  $\log T_{\text{eff}}$  (a) is estimated to be 0.01, and those in  $\log T_{\text{eff}}$  (b) is 0.02. Notice that the values of  $\log L$  derived by the two methods can differ by as much as 0.26, mainly due to differences in the adopted values of  $M_V$ , but that this difference is random in value and in direction. The major difference between the two methods is in the determination of the gravity or stellar mass. We adopted the mass from the evolutionary tracks, whereas in the non-LTE studies the mass was derived from the spectroscopic gravity. Notice that there are *systematic* differences between the gravity and mass derived by the two methods of

$$\log g(\text{spectr}) - \log g(\text{evol}) = -0.12 \pm 0.11 \quad (12)$$

and

$$\log M(\text{spectr}) - \log M(\text{evol}) = -0.13 \pm 0.11. \quad (13)$$

The masses derived from the spectroscopic gravity are on the average smaller than those derived from evolutionary tracks. The uncertainties in the gravities and masses derived spectroscopically are such that in most cases the masses are just within each others uncertainty limits. However, the systematic trend of

$M(\text{spectr})$  being smaller than  $M(\text{evol})$  suggests the presence of a real discrepancy between the two methods.

This mass difference has a large effect on the resulting values of  $v_{\text{esc}}$  because  $v_{\text{esc}} \sim M^{0.5} (1 - \Gamma)^{0.5}$  and  $\Gamma \sim M^{-1}$  (Table 4 columns 13–17). The lower spectroscopic masses produce values of  $v_{\text{esc}}$  which are systematically smaller than those derived from the evolutionary tracks by  $v_{\text{esc}}(\text{a})/v_{\text{esc}}(\text{b}) = 0.75 \pm 0.17$ . Since  $v_{\infty}$  is roughly proportional to  $v_{\text{esc}}$  a reduction of the values of  $v_{\text{esc}}(\text{b})$  adopted in this paper by a factor 0.75 would reduce the values of  $v_{\infty}(\text{pred})$  also by about a factor 0.75. Such a reduction would remove most of the discrepancy between  $v_{\infty}(\text{pred})$  and  $v_{\infty}(\text{obs})$ .

These considerations show the discrepancy can be removed by adopting the spectroscopic gravity and mass of the stars, rather than the higher evolutionary mass. There is a systematic difference between these two masses of  $M(\text{spectr})/M(\text{evol}) \simeq 0.74$ .

The evolutionary tracks after the core hydrogen phase are uncertain due to mass loss and overshooting so the evolutionary masses of the evolved stars might be in error. Moreover, we have assumed that the program stars are evolving away from the main sequence. The evolutionary tracks calculated by Maeder and Meynet (1987) show that stars with  $L > 6 \cdot 10^5 L_{\odot}$  will cross the region of the O-stars in the HR diagram twice; the second time with a mass which is a factor 0.6 lower than during the first crossing. So it is possible that some of the evolved stars have masses lower than we adopted from the evolutionary tracks. This effect may explain the discrepancy between  $M(\text{spectr})$  and  $M(\text{evol})$  for the evolved stars, and also the discrepancy between  $v_{\infty}(\text{pred})$  and  $v_{\infty}(\text{obs})$  for these stars.

However, we think that this is not the solution for the general discrepancy because we find about the same ratio  $v_{\infty}(\text{pred})/v_{\infty}(\text{obs}) \simeq 1.4$  independent of luminosity class, i.e., independent of the evolutionary stage. In particular, we find the same discrepancies between  $v_{\infty}(\text{obs})$  and  $v_{\infty}(\text{pred})$  and between  $M(\text{spectr})$  and  $M(\text{evol})$  for the class V stars as for the supergiants. This is a puzzling result because it implies that either the theoretical mass-luminosity relation of the upper main-sequence is wrong by about 30% in mass, or the prediction for the radiation driven winds are wrong by 40%.

**Table 3.** The predicted and observed terminal velocities as a function of luminosity class

| Luminosity class | Number of stars | $v_{\infty}(\text{pred})/v_{\infty}(\text{obs})$ | $v_{\infty}(\text{pred})/v_{\text{esc}}$ |
|------------------|-----------------|--|--|
| V                | 10              | $1.46 \pm 0.17$                                  | $3.87 \pm 0.22$                          |
| III              | 5               | $1.35 \pm 0.18$                                  | $3.90 \pm 0.19$                          |
| I                | 12              | $1.41 \pm 0.15$                                  | $3.85 \pm 0.08$                          |
| All              | 27              | $1.42 \pm 0.16$                                  | $3.87 \pm 0.16$                          |

**Table 4.** Comparison between the basic stellar parameters derived from non-LTE studies of the photospheric spectrum<sup>a</sup> and from evolutionary tracks<sup>b</sup>

| HD     | Type     | $\log L/L_{\odot}$ |          | $\log T_{\text{eff}}$ |       | $\log g$  |           | $\log M/M_{\odot}$ |           | $\log R/R_{\odot}$ |           | $\Gamma$ |      | $v_{\text{esc}}$ |      | $\frac{v_{\text{esc}}^{\text{a}}}{v_{\text{esc}}^{\text{b}}}$ | Ref. for a |
|--------|----------|--------------------|----------|-----------------------|-------|-----------|-----------|--------------------|-----------|--------------------|-----------|----------|------|------------------|------|---|------------|
|        |          | a                  | b        | a                     | b     | a         | b         | a                  | b         | a                  | b         | a        | b    | a                | b    |   |            |
| 93250  | O3V((f)) | 6.30±0.1           | 6.08±0.2 | 4.720                 | 4.686 | 3.95±0.15 | 3.98±0.13 | 1.97±0.18          | 1.92±0.10 | 1.23±0.05          | 1.19±0.13 | 0.57     | 0.38 | 950              | 1130 | 0.84  | 1          |
| 164794 | O4V((f)) | 6.03±0.1           | 6.02±0.2 | 4.699                 | 4.667 | 3.85±0.10 | 3.91±0.13 | 1.69±0.11          | 1.87±0.10 | 1.14±0.05          | 1.20±0.13 | 0.58     | 0.38 | 750              | 1050 | 0.71  | 2          |
| 93129A | O31f*    | 6.20±0.1           | 6.13±0.2 | 4.650                 | 4.648 | 3.60±0.15 | 3.78±0.13 | 1.74±0.18          | 1.92±0.10 | 1.32±0.05          | 1.29±0.13 | 0.77     | 0.43 | 480              | 960  | 0.50  | 1          |
| 66811  | O4I(n)f  | 6.00±0.1           | 5.87±0.2 | 4.623                 | 4.627 | 3.50±0.10 | 3.81±0.13 | 1.62±0.11          | 1.77±0.10 | 1.28±0.05          | 1.20±0.13 | 0.64     | 0.33 | 550              | 970  | 0.57  | 3          |
| 30614  | O9.5Ia   | 5.79±0.1           | 5.95±0.2 | 4.477                 | 4.490 | 2.90±0.10 | 3.11±0.13 | 1.50±0.11          | 1.71±0.10 | 1.46±0.05          | 1.52±0.13 | 0.52     | 0.46 | 450              | 560  | 0.80  | 2          |
| 37742  | O9.7Ib   | 5.74±0.1           | 5.74±0.2 | 4.505                 | 4.484 | 3.20±0.10 | 3.21±0.13 | 1.60±0.11          | 1.61±0.10 | 1.38±0.05          | 1.42±0.13 | 0.37     | 0.36 | 630              | 620  | 1.02  | 2          |
| 37128  | B0Ia     | 5.54±0.1           | 5.80±0.2 | 4.415                 | 4.447 | 2.75±0.10 | 3.00±0.13 | 1.37±0.11          | 1.62±0.10 | 1.46±0.05          | 1.53±0.13 | 0.39     | 0.40 | 430              | 530  | 0.81  | 4          |

<sup>a</sup> Basic parameters from detailed non-LTE studies.

<sup>b</sup> Basic parameters adopted here (mass from evolutionary tracks).

Ref. 1 = Simon et al. (1983)

Ref. 2 = Voels et al. (1988)

Ref. 3 = Kudritzki et al. (1983)

Ref. 4 = Kudritzki et al. (1988a)



We conclude that the discrepancy between  $v_{\infty}(\text{pred})$  and  $v_{\infty}(\text{obs})$  could be solved by adopting lower masses than those derived from evolutionary tracks for all luminosity classes. Such lower masses are suggested by the spectroscopic gravities.

We now investigate the influence of the adopted abundance and ionization on the predicted values of  $v_{\text{esc}}$  and  $v_{\infty}(\text{pred})$ . We adopted a standard He/H ratio of 0.1 by number, and assumed that H and He are fully ionized, i.e.,  $I_{\text{He}} = 2$  for the predictions of  $v_{\infty}$ . If the He/H ratio is larger than 0.1, which is possible in the evolved O If stars (e.g., Bohannan et al., 1986), or if He is not fully ionized, which is possibly the case in the winds of star cooler than O9, then the value of  $\Gamma$  would be smaller. For instance  $\Gamma$  decreases by 9% if helium is singly instead of fully ionized, and  $\Gamma$  decreases by 15% if helium is fully ionized and its abundance is increased from  $N(\text{He})/N(\text{H}) = 0.1$  to 0.3. So both effects would result in a decrease of  $\Gamma$  and an increase of  $v_{\text{esc}}$ . This would enhance rather than decrease the discrepancy between  $v_{\infty}(\text{obs})$  and  $v_{\infty}(\text{pred})$ .

We conclude that the uncertainty in the stellar abundances or in the degree of ionization in the wind cannot explain the systematic discrepancy of a factor 1.4 between  $v_{\infty}(\text{pred})$  and  $v_{\infty}(\text{obs})$  for main sequence stars, giants and supergiants.

### 5.2.2. Uncertainties in the force multiplier parameters

We now consider the effects of the uncertainty in  $\alpha$  and  $\delta$  on  $v_{\infty}$ .

In the analytic solution of the wind models by Kudritzki et al. (1988b) which we used here, the predicted values of  $v_{\infty}$  depend on  $\alpha$ ,  $\delta$  and on the stellar parameters  $L$ ,  $M$  and  $R$ . (In the self-consistent solution  $v_{\infty}$  depends *only* on the stellar parameters of course, because  $\alpha$  and  $\delta$  depend on  $L$ ,  $M$  and  $R$ .) This implies that the ratio  $v_{\infty}(\text{pred})/v_{\text{esc}}$  is not only a function of  $\alpha$  and  $\delta$  but depends also on the stellar parameters. In the range of the O-stars however, the ratio  $v_{\infty}(\text{pred})/v_{\text{esc}}$  is approximately constant (see Table 3). Therefore we will discuss the predictions and their sensitivity to  $\alpha$  and  $\delta$  in terms of  $v_{\infty}(\text{pred})/v_{\text{esc}}$ . Although this is not correct for each star individually, it is useful in showing the general trends of the comparison between  $v_{\infty}(\text{obs})$  and  $v_{\infty}(\text{pred})$ .

For the adopted values of  $\alpha = 0.695$  and  $\delta = 0.07$  at  $T_{\text{eff}} \geq 35,500$  and  $\delta = 0.03$  at  $T_{\text{eff}} < 35,500$  K we find a mean value of  $v_{\infty}(\text{pred})/v_{\text{esc}} = 3.87 \pm 0.16$  for all luminosity classes (Table 3). This value is much larger than the ratio  $v_{\infty}(\text{obs})/v_{\text{esc}} = 2.78 \pm 0.36$  (Eq. 6).

**Table 5.** The sensitivity of  $v_{\infty}/v_{\text{esc}}$  to  $\alpha$  and  $\delta$

| $\alpha$ | $\delta$ | $\langle v_{\infty}/v_{\text{esc}} \rangle^a$ |
|----------|----------|---|
| 0.695    | 0.035    | $4.2 \pm 0.3$                                 |
| 0.695    | 0.070    | $3.8 \pm 0.2$                                 |
| 0.695    | 0.105    | $3.2 \pm 0.2$                                 |
| 0.695    | 0.150    | $2.8 \pm 0.2$                                 |
| 0.600    | 0.070    | $2.6 \pm 0.2$                                 |
| 0.620    | 0.070    | $2.8 \pm 0.2$                                 |
| 0.695    | 0.070    | $3.8 \pm 0.2$                                 |
| 0.800    | 0.070    | $4.8 \pm 0.4$                                 |
| 0.640    | 0.100    | $2.8 \pm 0.2$                                 |

<sup>a</sup> This value and its error were calculated by averaging  $v_{\infty}/v_{\text{esc}}$  for our program stars.

We have tried to determine which set of force multiplier parameters would produce a ratio  $v_{\infty}(\text{pred})/v_{\text{esc}} = 2.8$  for our program stars. The result is given in Table 5. Notice that an increase of  $\delta$  reduces  $v_{\infty}/v_{\text{esc}}$ , whereas an increase of  $\alpha$  increases  $v_{\infty}/v_{\text{esc}}$ . The observed ratio  $v_{\infty}/v_{\text{esc}} \simeq 2.8$  can be reached by the following combinations of  $(\alpha, \delta) = (0.62, 0.07)$ ,  $(0.64, 0.10)$  or  $(0.695, 0.15)$  and possibly others. These combinations do not agree with the calculated values of  $\alpha$  and  $\delta$  for O-stars, in LTE or in non-LTE, shown in Fig. 6. We conclude that the available calculations of the force multiplier parameter, even those in which non-LTE effects and multiple line effects are taken into account do not reproduce the observed values of  $v_{\infty}$  for O-stars, for the adopted stellar parameters. If the adopted stellar parameters are correct and  $\delta \simeq 0.07$ , a value of  $\alpha \simeq 0.62$  to 0.64 is required to match the observed and predicted terminal velocities.

## 6. Discussion and conclusions

We have derived the terminal and turbulent velocities of the stellar winds of 27 O-type stars from a comparison between the observed UV resonance lines and theoretical profiles, calculated with the SEI-method. The wind is assumed to be stationary and spherically symmetric with a monotonically increasing velocity law. The velocity law and the turbulent velocity are derived from the linefits. In this study the turbulent velocity is assumed to be constant and represented by a Gaussian broadening profile. The real nature of the broadening mechanism in the winds of the O-stars is unknown. Lucy (1984) suggested that the broadening is due to radiation driven shocks in the wind. In that case one expects the shocks to occur in the region of the wind where the main acceleration occurs. The observations indicate that the broadening occurs over the full velocity range of the wind from  $v \simeq 0$  to  $v_{\infty}$  (see Introduction). Therefore we assumed as a first order approximation that the turbulent velocity is constant throughout the wind. So the value of  $v_{\text{turb}}$  derived for each star in this paper should be considered as mean value of the “turbulence” throughout the wind of that star. We have assumed that the broadening mechanism in the winds of O-stars can be represented by isotropic Gaussian turbulence. This may be a severe oversimplification. For instance, if the broadening is due to radiation driven shocks, the broadening will be mainly in the radial direction from the star. Fortunately, the assumption of isotropic broadening will not introduce a significant error in the determination of  $v_{\infty}$ . The reason for this is that the turbulent velocity is derived predominantly from the fitting of the absorption part of the line profile which is sensitive to the radial component of the turbulence. So the derived value of  $v_{\text{turb}}$  is the mean value of the radial component of the broadening mechanism in the wind.

When better predictions for the nature of the broadening mechanism and its variation with height and directional amplitude become available, these can be easily taken into account in the SEI method. In this study of the terminal velocity of the winds of O-stars the lack of understanding of the true nature of the broadening does not affect the conclusions.

We found from the linefitting that the mean turbulent velocity of the winds of O-stars range from 150 to 300 km s<sup>-1</sup>.

The terminal velocities of stellar winds derived in this paper are smaller than those estimated on the basis of the edge velocity of the UV resonance lines and those derived from the linefitting with the Sobolev method by about 400 km s<sup>-1</sup> (Fig. 2). This is due to the effect of the turbulence, which shifts the short wavelength

edge of the lines to velocities more negative than  $-v_\infty$ . Since this effect is not taken into account in the linefitting with the Sobolev method, the values of  $v_\infty$  derived from Sobolev profiles are generally overestimated.

The terminal velocities scale with the escape velocities as  $v_\infty \simeq 2.8 v_{\text{esc}}$  (Eq. 6) for the O-stars with some weak evidence that the ratio  $v_\infty/v_{\text{esc}}$  decreases with temperature from 3.2 at  $\log T_{\text{eff}} = 4.60$  to 2.8 at  $\log T_{\text{eff}} = 4.50$ . [It is amusing to see that the present value of  $v_\infty/v_{\text{esc}} = 2.78$  is the same as the very first estimate of this ratio  $v_\infty/v_{\text{esc}} = 2.8$  based on the observations of six stars in the epoch before the Copernicus satellite and IUE (Lamers et al., 1976).]

The observed values of  $v_\infty$  are compared with the predictions from the radiation driven wind theory in which non-LTE effects and the effects of multiline scattering are taken into account, using the analytical solutions of the wind models by Kudritzki et al. (1988b) (Sect. 5). The predictions overestimate  $v_\infty$  by about 40% for all luminosity classes (Table 3 and Fig. 7).

At first glance our results seem to contradict those of Puls (1987) who found a very good agreement between the predicted and observed value of  $v_\infty \simeq 2200 \text{ km s}^{-1}$  for the star  $\zeta$  Pup based on self-consistent calculations of the stellar wind. These calculations showed that  $\alpha = 0.685$  and  $\delta = 0.072$ , i.e., very similar to the values we adopted! The difference between Puls' value of  $v_\infty$  (pred) =  $2140 \text{ km s}^{-1}$  and our value of  $v_\infty$  (pred) =  $3690 \text{ km s}^{-1}$  is due to the difference in the adopted stellar parameters. Puls adopted a radius of  $22 R_\odot$  which is larger than the value of  $18 R_\odot$  derived from the distance modulus and the non-LTE analysis of the photospheric spectrum by Bohannan et al. (1986) and larger than our value of  $16 R_\odot$ . The larger radius implied a higher luminosity of  $\log L = 6.13$  compared to our value of  $\log L = 5.87$ . Moreover, Puls adopted a mass of  $56 M_\odot$  derived from the spectroscopic gravity and the radius, which is lower than the evolutionary mass of  $80 M_\odot$  for this luminosity, if the star evolves away from the main sequence. The higher luminosity and the lower mass adopted by Puls result in a value of  $v_{\text{esc}} = 600 \text{ km s}^{-1}$  which is much lower than our value of  $970 \text{ km s}^{-1}$ . This explains the difference between Puls' and our values of  $v_\infty$  (pred).

A simple test shows that an increase of the distance modulus of all stars by as much as 0.5 and the corresponding increase in  $L$  by a factor 1.58 and in  $R$  by a factor 1.25 reduces  $v_{\text{esc}}$  and  $v_\infty$  (pred) by less than 15%. This is due to the fact that the increase in  $L$  is largely compensated by the increase in the evolutionary mass. It is unlikely that the distance moduli of all clusters are underestimated by more than about 0.5 magnitudes.

A detailed comparison of the stellar parameters derived from spectroscopic non-LTE studies with those adopted here shows that the spectroscopic gravities and masses are systematically lower than those derived from the evolutionary tracks by about a factor 0.75. If the spectroscopic masses are adopted the values of  $v_\infty$  (pred) agree with  $v_\infty$  (obs) (Sect. 5.2.1). This suggests that either the spectroscopic masses or the evolutionary masses are systematically in error. If the discrepancy between  $v_\infty$  (obs) and  $v_\infty$  (pred) is due to errors in the evolutionary mass (i.e., derived from  $L$  and  $T_{\text{eff}}$ ), then the fact that we found the same discrepancies in  $v_\infty$  for all luminosity classes suggests that the evolutionary masses of the main-sequence stars are also wrong. This would be surprising as there is no obvious explanation for this effect.

The predicted values of  $v_\infty$  depend strongly on the force multiplier parameters  $\alpha$  and  $\delta$  which were taken from recent

calculations by Pauldrach et al. (1988). These calculations include detailed non-LTE statistical equilibrium calculations for more than  $10^5$  lines of H to Zn with solar abundances (Holweger, 1979). The calculations predict  $\alpha \simeq 0.695$  and  $\delta \simeq 0.07$  if  $T_{\text{eff}} \geq 35,500 \text{ K}$  and  $\delta \simeq 0.03$  if  $T_{\text{eff}} < 35,500 \text{ K}$  (Sect. 5.1) with a small scatter for the individual models. In order to bring the values of  $v_\infty$  (obs) and  $v_\infty$  (pred) into agreement,  $\alpha$  has to be decreased to 0.62 or  $\delta$  should be increased to 0.15. Of course a combination of other values of  $\alpha$  and  $\delta$  may also bring the velocities into agreement (Sect. 5.2). At present we do not know if such adjustments of  $\alpha$  and  $\delta$  are possible within the framework of the relevant theories. Puls (1987) has shown that the values of  $\alpha$  are rather insensitive to changes in the structure of the wind model for the star  $\zeta$  Pup and ranges from  $\alpha = 0.685$  to 0.709 for a variety of wind models from isothermal to non-isothermal winds. The value of  $\delta$  however is sensitive to energy distribution of the lower boundary photospheric model:  $\delta \simeq 0.11$  and 0.07 for LTE and non-LTE model atmospheres respectively. Since the non-LTE energy distributions are more appropriate than the LTE ones, the lower values of  $\delta$  are preferred, and thus the discrepancy remains.

If the discrepancy between  $v_\infty$  (obs) and  $v_\infty$  (pred) is due to errors in the coefficients  $\alpha$  and  $\delta$  describing the force multiplier, then this study indicates that the presently available self-consistent non-LTE wind models are not fully adequate in describing the physical processes in the winds of O-stars. Several effects which might alter the values of  $\alpha$  and  $\delta$  can be suggested: different ionization structure, different abundances, shocks in the winds, turbulence in the winds, and rotation. At present it is not clear which of these effects, if any, would change the values of  $\alpha$  and  $\delta$  in the direction suggested by the observed terminal velocities (Sect. 5.2.2).

The reduction of  $v_\infty$  of O-stars by about  $400 \text{ km s}^{-1}$  relative to previous determinations has interesting consequences for the explanation of the narrow absorption components (NAC) which are often observed in the UV resonance lines. Lamers et al. (1982) have shown that the NAC occur preferentially at a velocity of 0.7 to  $0.8 v_\infty$ . If we now take into account the reduction of  $v_\infty$ , the velocities of the NAC come close to the terminal velocity. This is supported by a recent study of the variability of the NAC's in  $\zeta$  Per (HD 24912) and  $\lambda$  Cep (HD 210839) by Henrichs et al. (1988). They find that the variable NAC always accelerate to the same final velocity of  $2200 \text{ km s}^{-1}$  for  $\zeta$  Per and  $2010 \text{ km s}^{-1}$  for  $\lambda$  Cep, and they argue that this final velocity is in effect the terminal velocity of the wind. This is supported by our results which show from an accurate linefit of the UV resonance lines that  $v_\infty = 2400 \pm 100 \text{ km s}^{-1}$  for  $\zeta$  Per and  $2100 \pm 60 \text{ km s}^{-1}$  for  $\lambda$  Cep.

**Acknowledgements.** We thank the Astronomical Data Center of NASA Goddard Space Flight Center for providing us with the magnetic tape of the IUE atlas of Walborn et al. (1985) which was essential for this study. The second author is grateful to P. Conti, C. Garmany and T. Snow for hospitality at JILA and CASA (Boulder) in the summer of 1988 where part of this study was carried out. We thank P. Conti, C. Garmany, D. Hummer, R. Kudritzki and J. Puls for critical discussions and comments. We thank the staff of the JILA Scientific Reports Office for preparing the manuscript. This research was partly supported National Science Foundation grant AST-88-06594, by NASA grant NSG-5300 to the University of Colorado and by the Deutsche Forschungsgemeinschaft under grant KU 474-1113.

## References

- Abbott, D.C.: 1978, *Astrophys. J.* **225**, 893  
 Abbott, D.C.: 1982, *Astrophys. J.* **259**, 282  
 Bohannan, B., Abbott, D.C., Hummer, D.G., Voels, S.A.: 1986, in *Luminous Stars and Associations in Galaxies*, eds. C. de Loore, A. Willis, P. Laskarides, Reidel, Dordrecht, p. 111  
 Cassinelli, J.P., Lamers, H.J.G.L.M.: 1987, in *Scientific Accomplishments of IUE*, eds. Y. Kondo et al., Reidel, Dordrecht, p. 139  
 Castor, J.I., Abbott, D.C., Klein, R.I.: 1975, *Astrophys. J.* **195**, 157  
 Castor, J.I., Lamers, H.J.G.L.M.: 1979, *Astrophys. J. Suppl.* **39**, 481  
 Chiosi, C., Nasi, E., Sreenivasan, S.R.: 1978, *Astron. Astrophys.* **73**, 103  
 Chlebowski, T., Garmany, C.D.: 1988, in preparation  
 Garmany, C.D.: 1987, private communication  
 Garmany, C.D., Conti, P.S., Chiosi, C.: 1982, *Astrophys. J.* **263**, 777  
 Groenewegen, M.A.T., Lamers, H.J.G.L.M.: 1989, in press (Paper I)  
 Hamann, W.R.: 1980, *Astron. Astrophys.* **84**, 342  
 Hamann, W.R.: 1981, *Astron. Astrophys.* **93**, 353  
 Henrichs, H.F., Kaper, L., Zwarthoed, G.A.A.: 1988, in *Proceedings of the 10th IUE Meeting* (preprint)  
 Holweger, H.: 1979, *Les elements et leur isotopes dans l'univers*, Université de Liège, Institut d'Astrophysique  
 Howarth, I.D., Prinja, R.K.: 1989, *Astrophys. J. Suppl.* **69**, 527  
 Humphreys, R.M.: 1978, *Astrophys. J. Suppl.* **38**, 309  
 Humphreys, R.M., McElroy, D.B.: 1984, *Astrophys. J.* **284**, 565  
 Kudritzki, R.P., Simon, K.P., Hamann, W.R.: 1983, *Astron. Astrophys.* **118**, 245  
 Kudritzki, R.P., Gabler, A., Gabler, R., Groth, H.G., Pauldrach, A.W.A., Puls, J.: 1988a, in *Physics of Luminous Blue Variables*, eds. K. Davidson et al., Kluwer, Dordrecht (in press)  
 Kudritzki, R.P., Pauldrach, A., Puls, J., Abbott, D.C.: 1988b, preprint  
 Lamers, H.J.G.L.M., Gathier, R., Snow, T.P.: 1982, *Astrophys. J.* **258**, 186  
 Lamers, H.J.G.L.M., Cerruti-Sola, M., Perionotto, M.: 1987, *Astrophys. J.* **314**, 726  
 Lamers, H.J.G.L.M., Rogerson, J.B.: 1978, *Astron. Astrophys.* **66**, 417  
 Lamers, H.J.G.L.M., van de Heuvel, E.P.J., Petterson, J.: 1976, *Astron. Astrophys.* **49**, 327  
 Lucy, L.B.: 1983, *Astrophys. J.* **274**, 392  
 Lucy, L.B.: 1984, *Astron. Astrophys.* **140**, 210  
 Maeder, A., Meynet, G.: 1987, *Astron. Astrophys.* **182**, 243  
 Pauldrach, A., Kudritzki, R.P., Puls, J., Butler, K.: 1988, *Astron. Astrophys.* (submitted)  
 Pauldrach, A., Puls, J., Kudritzki, R.P.: 1986, *Astron. Astrophys.* **164**, 86  
 Prinja, R.K.: 1985, Thesis, University College London  
 Puls, J.: 1987, *Astron. Astrophys.* **184**, 227  
 Simon, K.P., Jonas, G., Kudritzki, R.P., Rahe, J.: 1983, *Astron. Astrophys.* **125**, 34  
 Snow, T.P., Morton, D.C.: 1976, *Astrophys. J. Suppl.* **32**, 429  
 Voels, S.A., Bohannan, B., Abbott, D.C., Hummer, D.G.: 1988, *Astrophys. J.* (in press)  
 Walborn, N.R., Nichols-Bohlin, J., Panek, R.J.: 1985, NASA Reference Publication 1155: International Ultraviolet Explorer atlas of O-type Spectra from 1200 to 1900 Å